ELSEVIER

Chemical Engineering Journal 133 (2007) 105–111

Chemical Engineering Journal

www.elsevier.com/locate/cej

Fluid segment configuration for improving product yield and selectivity of catalytic surface reactions in microreactors

Nobuaki Aoki, Kunio Yube, Kazuhiro Mae *

Department of Chemical Engineering, Graduate School of Engineering, Kyoto University, Kyoto-daigaku Katsura, Nishikyo-ku, Kyoto 615-8510, Japan

Received 27 August 2006; received in revised form 8 February 2007; accepted 13 February 2007

Abstract

Ordered laminar flow and mixing driven mainly by molecular diffusion in microreactors enables operation using fluid segments. This paper discusses the effects of configuration of fluid segments including reactants at the reactor inlet for catalytic surface reactions in a microreactor. Irreversible and reversible parallel and series–parallel reaction systems were investigated. The rate-controlling step of these reaction systems is diffusion in the channel or diffusion in the catalyst layer. Under some diffusion-controlled conditions, appropriate fluid segment configuration gives higher selectivity of the desired product than reactors where the reactants are mixed at the reactor inlet. Configurations in which reactants with different reaction orders in parallel reactions or consumed only in the reaction producing the desired product are placed on the catalyst surface are suitable to improve the selectivity of the desired product. The configuration to maximize the yield of the desired product depends on the reaction system and rate-controlling step. To obtain a given selectivity of the desired product, the required fluid segment size depends on the configuration. The results reported here indicate an advantage of fluid segment, which is a typical fluid operation in microreactors, for enhancing the yield and selectivity of desired products.

Keywords: Catalytic surface reaction; Microreactor; Yield and selectivity; Fluid segment; Reaction order

1. Introduction

Microreactors are miniaturized reactors including microchannels with characteristic dimensions in the sub-millimeter range. Channel miniaturization provides a high surface-to-volume ratio and laminar flow [1,2]. High surface-to-volume ratios lead to enhanced heat and mass transfer, and thus lead to efficient catalytic surface reactions. Examples of catalytic surface reactions in microreactors are as follows: ammonia oxidation on a platinum catalyst [3], degradation of 4-chlorophenol on titanium dioxide as a photocatalyst [4], methanol steam reforming using a $CuO/ZnO/Al_2O_3$ catalyst [5], production of hydrogen from ammonia on alumina [6], reforming/oxidation of methanol on thin metallic wires containing Cu and Zn [7], and 1-pentene epoxidation on a TS-1 (titanium silicalite-1) catalyst [8]. Numerical investigations of catalytic surface reactions in microreactors have also been performed [9,10].

Laminar flow leads to mixing driven mainly by molecular diffusion. The mixing time by molecular diffusion scales with the square of diffusion length. Therefore, a short diffusion length is necessary for rapid mixing. Mixing operations by which reactant fluids are separated into many micro fluid segments are often used for this purpose. Examples of the micromixers using this mixing principle include the interdigital mixer [11], the static V-micro-jetmixer [12], the SuperFocus mixer [13], the K-M mixer (Kyoto University-MCPT; Research Association of Micro Chemical Process Technology) [14,15], and the dual pipe mixer [16]. To achieve efficient mixing realizing controlled reaction conditions, we have proposed guidelines to determine design factors of fluid segment, such as width, arrangement, and shape using dimensionless numbers representing the ratio of reaction rate to mixing rate and the ratio of the diffusion rates in the horizontal and vertical directions in the cross-section of a reactor [17,18].

We have also examined the effects of fluid segment configuration, *i.e.*, combinations of reactant concentrations, width, and arrangement of laminated fluid segments on product distribution of multiple reactions [19]. For the fixed mean fluid segment size, the selectivity of the desired product for series–parallel

* Corresponding author. Tel.: +81 75 383 2668; fax: +81 75 383 2658.
E-mail address: kaz@cheme.kyoto-u.ac.jp (K. Mae).

1385-8947/$ – see front matter © 2007 Elsevier B.V. All rights reserved.
doi:10.1016/j.cej.2007.02.006

reactions depends on the configuration. Ordered laminar flow and mixing driven by molecular diffusion enables this operation.

In catalytic surface reactions, the reactions occur only in the catalyst layer. The concentration profile near the catalyst layer dominates the product distribution in a reactor. Configuration of reactants at the reactor inlet is expected to enable the concentration of reactants on the catalyst surface to be controlled and thus to be useful to improve yield and selectivity of the desired products in such reactions. To establish the effectiveness of fluid segment configuration in catalytic surface reactions, we investigated the effects of the arrangement of fluid segments including reactants at the reactor inlet for catalytic surface reactions in microchannels. We applied irreversible and reversible parallel and series–parallel reaction systems proceeding in the channel between two parallel plates into CFD (computational fluid dynamics) simulations. We also examined the effects of the following rate-controlling steps of the reaction systems: surface diffusion and diffusion in the catalyst layer. Moreover, we studied the effects of fluid segment size on the selectivity of the desired product and discuss channel size to achieve a certain yield of the desired product for each fluid segment configuration.

2. Simulation settings

First, the settings for all CFD simulations in this study are explained. We simulated mixing by molecular diffusion, reaction, and flow in reactors with a channel between two parallel plates of width W (two-dimensional simulations) and various configurations of fluid segments that will be described in the subsequent sections. A commercial CFD code, Fluent 6.2.16, was used for the CFD simulations. This code solves mass, momentum, and energy conservation equations by the control volume method [20]. The laminar flow and the finite-rate model were applied. The SIMPLE (semi-implicit method for pressure-linked equations) algorithm was used to solve the pressure–velocity coupling equation. The second-order upwind scheme was used to solve mass and momentum conservation equations. The discretization method of the simulation domain is mentioned in subsequent sections. We confirmed that the solutions of the CFD simulations are independent of the further increase in number of mesh elements.

The diffusion coefficient of every species D was assumed to be $10^{-9}\,\mathrm{m^2\,s^{-1}}$, which is the typical order of the diffusion coefficients for liquid phase reactions [21]. The physical properties of the two-reactant fluids are as follows: the density is $1000\,\mathrm{kg\,m^{-3}}$, and the viscosity is 0.001 Pa s. The inlet velocity of the reactant fluids u was fixed at $0.001\,\mathrm{m\,s^{-1}}$.

Using the settings described in the following sections, we performed CFD simulations to obtain concentration profiles of the species in the reactors and then calculated relations between the yield of the desired product C, Y_C, and conversion of the reactant B, x_B, in the reactors as a measure of reactor performance. These relations were obtained from the mass-weighted average concentration of each species on the plane perpendicular to the axial direction at each axial position.

2.1. Effects of fluid segment configurations for each multiple reaction system

Fig. 1 shows a schematic of the reactor channel and simulation settings applied in the CFD simulations with various reaction systems. Diffusion from the reactor channel to the catalyst surface was assumed to be the rate-controlling step. The catalyst is loaded on the bottom of the channel and this is where the reactions take place. Analogous catalyst loading is realized by placing a membrane catalyst on the bottom of the reactor channel [22]. The no-slip boundary condition was assumed on both channel walls. The reaction formulas and the rate equations of the multiple reactions proceeding in the reactors were as follows:

(1) Parallel reactions (irreversible),

$$\mathrm{A + B \rightarrow C}, \quad r_1 = k_1 C_A C_B,$$
$$\mathrm{A + B \rightarrow D}, \quad r_2 = k_2 C_A C_B^{0.5}, \tag{1}$$

where $k_1 = 1\,\mathrm{m^4\,kmol^{-1}\,s^{-1}}$ and $k_2 = 0.1\,\mathrm{m^{2.5}\,kmol^{-0.5}\,s^{-1}}$;

(2) Parallel reactions (reversible),

$$\mathrm{A + B \rightleftarrows C}, \quad r_1 = k_1 C_A C_B - k_{-1} C_C,$$
$$\mathrm{A + B \rightleftarrows D}, \quad r_2 = k_2 C_A C_B^{0.5} - k_{-2} C_D, \tag{2}$$

where $k_1 = 1\,\mathrm{m^4\,kmol^{-1}\,s^{-1}}$, $k_2 = 0.1\,\mathrm{m^{2.5}\,kmol^{-0.5}\,s^{-1}}$ and $k_{-1} = k_{-2} = 0.01\,\mathrm{m\,s^{-1}}$;

(3) Series–parallel reactions,

$$\mathrm{A + B \rightarrow C}, \quad r_1 = k_1 C_A C_B,$$
$$\mathrm{B + C \rightarrow D}, \quad r_2 = k_2 C_B C_C, \tag{3}$$

where $k_1 = 1\,\mathrm{m^4\,kmol^{-1}\,s^{-1}}$ and $k_2 = 0.1\,\mathrm{m^4\,kmol^{-1}\,s^{-1}}$.

In the reaction formulas, A and B are the reactants, C is the desired product, D is the by-product, r_i and k_i are the reaction rate ($\mathrm{kmol\,m^{-2}\,s^{-1}}$) and the rate constant of the ith reaction, respectively, and C_j is the molar concentration of the species j. The reactants were assumed to react isothermally, and the rate constants were fixed. The reaction order of B for the reaction producing C was higher than that for the reaction producing D. The channel width was 200 μm, which is of the typical order of microchannel size [23]. The channel width affects the rate-controlling step. The reactor length L was set to 0.1 m, *i.e.*, the mean residence time of the reactants in the reactors τ was

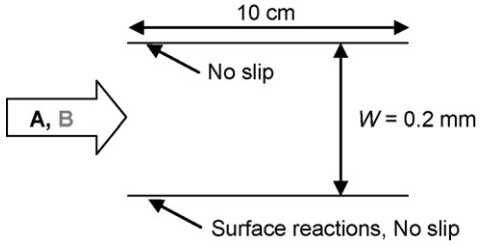

Fig. 1. Simulation settings of the reactor under channel diffusion-controlled conditions.

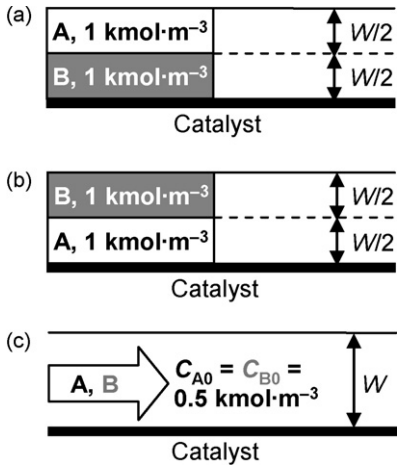

Fig. 2. Configurations of fluid segments: (a) AB-cat, (b) BA-cat, and (c) mixed. Each fluid segment width is half the channel width. In mixed, A and B are mixed at the reactor inlet.

100 s. The vessel dispersion number $D/uL \leq 10^{-5}$, and thus the influence of axial dispersion was negligible [24].

Fig. 2 shows the configurations of fluid segments of the reactants. In configuration AB-cat, B is placed on the surface of the catalyst layer, while in configuration BA-cat, A is placed on the surface of the catalyst layer, and in configuration mixed, the two reactants are mixed at the reactor inlet. The concentrations of A and B in each fluid segment were both set at 1 kmol m^{-3} in configurations AB-cat and BA-cat, while in configuration mixed, the reactant concentrations in the reactant fluid were set at 0.5 kmol m^{-3}. Thus, the mean initial concentrations of the reactants for all configurations were $C_{A0} = C_{B0} = 0.5$ kmol m^{-3}, and the molar flows of each reactant at the reactor inlet were equivalent. The concentrations were selected to adjust the reaction rates so that the diffusion from the channel to the catalyst layer was the rate-controlling step. The fluid segment size is half of the channel width, *i.e.*, 100 μm. The calculation domain was discretized by the rectangular mesh, and the number of mesh elements was 19,200.

2.2. Effects of fluid segment configurations for reaction systems the rates of which are controlled by diffusion in the catalyst layer

We then studied the effects of fluid segment configurations for each rate-controlling step. Fig. 3a shows the reactor model for the reaction system the rate of which is controlled by diffusion in the catalyst layer. The two reactions shown in Eq. (1) took place on the bottom of the catalyst layer. The channel width was 200 μm, and the thickness of catalyst layer was 400 μm. The thickness of the catalyst layer was greater than the channel width, and thus the diffusion in the catalyst layer was the rate-controlling step.

Fig. 3b shows the reactor model for the reaction system in which the first reaction in Eq. (1) is controlled by diffusion in the catalyst layer as well as diffusion in the reactor channel. The first reaction producing C occurs near the bottom of the catalyst layer (r_1 (kmol m^{-3} s^{-1}) $= k_1 C_A C_B$,

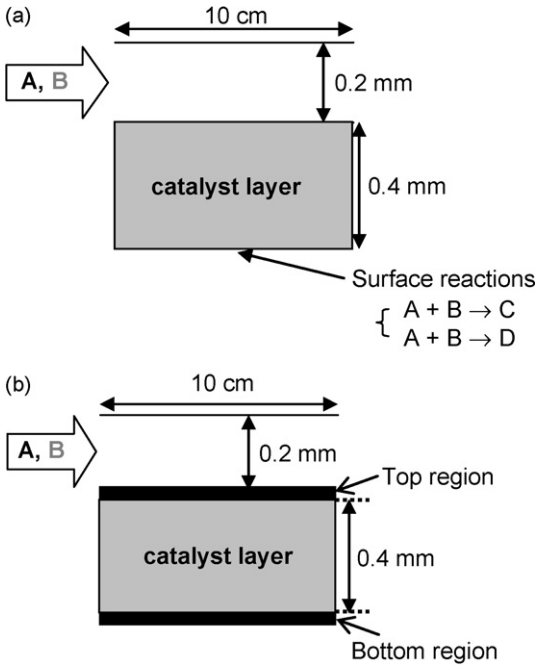

Fig. 3. Settings of the reactors under conditions in which the rate is controlled by diffusion in the catalyst layer. (a) Both reactions proceed at the bottom of the catalyst layer. (b) The reaction producing D (A + B → D) occurs in the top region, and the reaction producing C (A + B → C) occurs in the bottom region. The thicknesses of the top and bottom regions are 0.01 mm. In the catalyst layer and the top and bottom regions, each species moves only by molecular diffusion.

$k_1 = 10^3$ m^3 kmol^{-1} s^{-1}), and the second reaction producing D occurs near the channel surface (r_2 (kmol m^{-3} s^{-1}) $= k_2 C_A C_B^{0.5}$, $k_2 = 10^2$ m$^{1.5}$ kmol$^{-0.5}$ s^{-1}). Thus, the diffusion length for producing C is longer than that for producing D. The thickness of the region for producing each product was set at 10 μm, and that of the catalyst layer was 400 μm. The TS-1 catalyst is considered to have internal and external catalytic cites [25]. When the catalyst is used for the oxidation of phenol with hydrogen peroxide, catechol is mainly produced on the external catalytic cites, and hydroquinone is mainly produced on the internal catalytic cites.

The common settings for both reaction systems were as follows. In the catalyst layer, the species were assumed to move only by molecular diffusion: *i.e.*, the flow velocity was 0 m s^{-1}. The diffusion coefficient was set at 10^{-9} m^2 s^{-1} in the entire reactor region. The two reactants were fed into the channel in the three configurations shown in Fig. 2. The reactor length L was set at 0.1 m, *i.e.*, the mean residence time of the reactants in the reactors τ was 100 s. The calculation domain was discretized by the rectangular mesh, and the number of mesh elements was 36,000 for the reaction system shown in Fig. 3a and 30,800 for that shown in Fig. 3b.

2.3. Effects of fluid segment size

We also examined the effects of fluid segment size for each fluid segment configuration. We changed W to 2 or 2000 μm, in addition to 200 μm examined in Section 2.1. The size of fluid segments was $W/2$. The parallel reactions

shown in Eq. (1) occurred in the reactors. Diffusion from the reactor channel to the catalyst surface was assumed to be the rate-controlling step. The reactor length L was set at 0.001 m for $W = 2\,\mu m$ and at 10 m for $W = 2000\,\mu m$: *i.e.*, the mean residence time of the reactants in the reactors τ was 1 s for $W = 2\,\mu m$ and 10,000 s for $W = 2000\,\mu m$. The vessel dispersion number $D/uL \leq 10^{-3}$, and thus the influence of axial dispersion is negligible [23]. The calculation domain was discretized by the rectangular mesh, and the number of mesh elements was 19,200.

3. Results and discussion

3.1. Effects of fluid segment configurations for each multiple reaction

3.1.1. Parallel reactions (irreversible)

Fig. 4 shows the effects of fluid segment configuration on the yield of C for the irreversible parallel reactions. At the same conversion of B, a higher yield of C is equivalent to higher selectivity of C. Configuration AB-cat gave the highest Y_C among the three configurations tested. This tendency can be explained as follows. In this reaction system, the reaction order of B for producing C is greater than that for producing D. A high concentration of B on the catalyst surface is desirable to increase Y_C. In configuration AB-cat, B is placed near the catalyst surface, and the surface concentration of B is thus the highest among the three configurations tested, as shown in Fig. 5. Based on the simulation results, we concluded that under diffusion-controlled conditions, a proper fluid segment configuration gives higher yield and selectivity of the desired product than the reactor where the reactants are mixed at the reactor inlet.

From the results presented in this section, we can infer a suitable reactant distribution in a channel the channel shape of which is different from the parallel plates where the catalyst is loaded on only one plate. As an example, we consider a circular tube reactor the walls of which are coated with a catalyst. The reactant with reaction orders that are different in parallel reactions should be distributed near the channel wall, and the other reactant should be located in the center of the channel. This distribution is realized by a dual coaxial pipe.

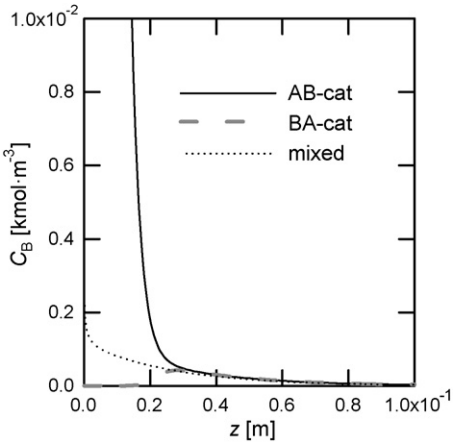

Fig. 5. Concentration of B on the catalyst surface for each configuration as a function of axial position z (m) (irreversible parallel reactions).

3.1.2. Parallel reactions (reversible)

Fig. 6 shows Y_C of each fluid segment configuration for the reversible parallel reactions. The tendency of Y_C in these configurations is analogous to that in the irreversible reactions. However, the difference in Y_C is smaller for the reversible than for the irreversible reactions. This small difference is attributed to the surface concentrations of the species. The reactions were assumed to be so fast that they reached equilibrium rapidly, resulting in a fixed concentration of each species on the catalyst surface. This is especially the case for configuration mixed. After a certain axial position, the surface concentrations of species are kept constant, as shown in Fig. 7. Thus, the effect of fluid segment configurations on Y_C is small.

3.1.3. Series–parallel reactions

Fig. 8 shows the effects of fluid segment configuration on the yield of C for the series–parallel reactions. In this reaction system, configuration BA-cat gave the highest Y_C. Reactant A was

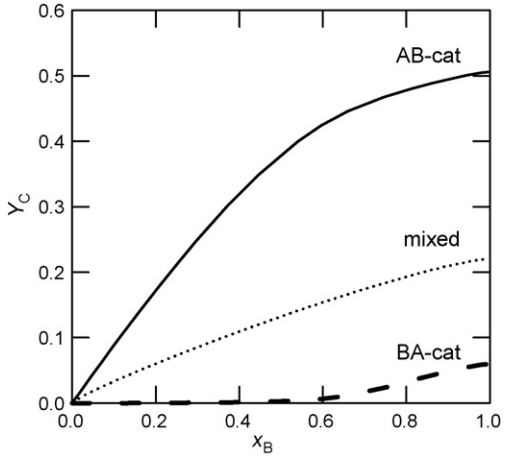

Fig. 4. Yields of the desired product in the irreversible parallel reactions for each fluid segment configuration.

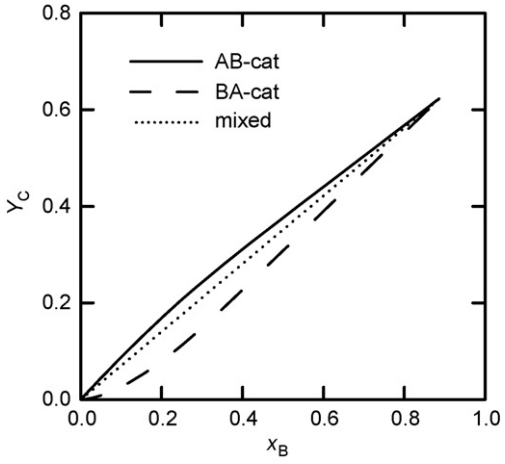

Fig. 6. Yields of the desired product in the reversible parallel reactions for each fluid segment configuration.

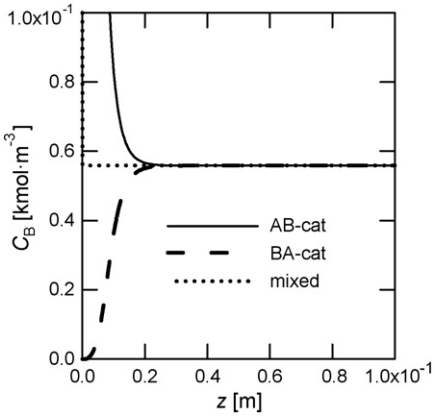

Fig. 7. Concentration B on the catalyst surface for each configuration as a function of axial position z (m) (reversible parallel reactions).

used to only produce C, while reactant B was used to consume D as well as to produce C. To slow the reaction consuming D, a configuration where B is subject to a greater degree of diffusion control than A is preferable. The results of the reaction systems shown in Eqs. (1)–(3) indicate that the arrangement to maximize the desired product yield is dependent on the reaction system.

3.2. Effects of fluid segment configurations for the reaction system the rate of which is controlled by diffusion in the catalyst layer

3.2.1. The two reactions occur on the bottom of the catalyst layer

Fig. 9 shows the yields of C for the irreversible parallel reactions that occur on the bottom of the catalyst layer. The tendency of Y_C according to the configurations was analogous to that in the reaction system the rates of which are controlled by diffusion from the channel to the catalyst surface. However, the difference in Y_C for the reactions occurring on the bottom of the catalyst layer was smaller than those on the top of the catalyst layer. This is because the ratio of diffusion length from the channel to the catalytic layer for the reactions of B to that of A becomes small when the reactions occur on the bottom of the catalyst

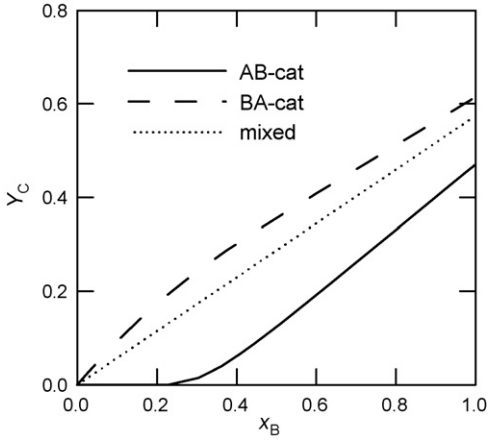

Fig. 8. Yields of the desired product in the series–parallel reactions for each fluid segment configuration.

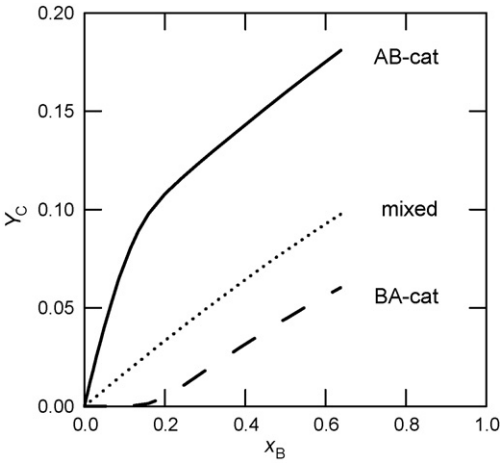

Fig. 9. Yields of the desired product in the reaction system the rate of which is controlled by diffusion in the catalyst layer. The two reactions occur on the same plane.

layer. Thus, the effect of the configurations is minimized when the diffusion in the catalyst layer controls the reaction rate.

3.2.2. The two reactions occur in different regions of the catalyst layer

Fig. 10 shows Y_C for the irreversible parallel reactions that occur on the top (producing D) and bottom (producing C) of the catalyst layer. As the diffusion length for producing the desired product is much longer than that for the by-product, the yield of C is very small. For the reaction producing C to proceed, both reactants must reach the bottom of the catalyst layer. In this reaction system, diffusion of both reactants to this region is the rate-controlling step. Thus, configuration mixed enables the fastest transfer of both reactants to this region among the three configurations tested, and this configuration therefore yields the highest Y_C among the three configurations. The results described in this section indicate that the rate-controlling step also affects the most suitable configuration for maximizing the desired product yield and selectivity.

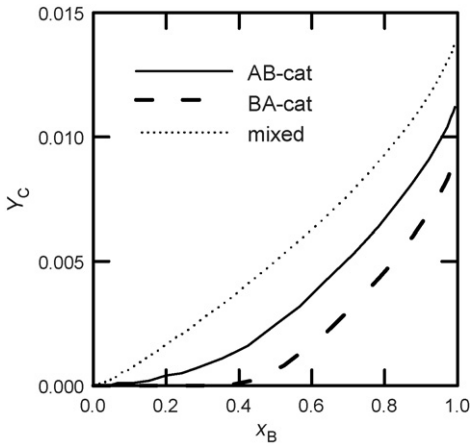

Fig. 10. Yields of the desired product in the reaction system the rate of which is controlled by diffusion in the catalyst layer. The reaction producing D occurs near the surface of the catalyst layer, and the reaction producing C occurs near the bottom of the catalyst layer.

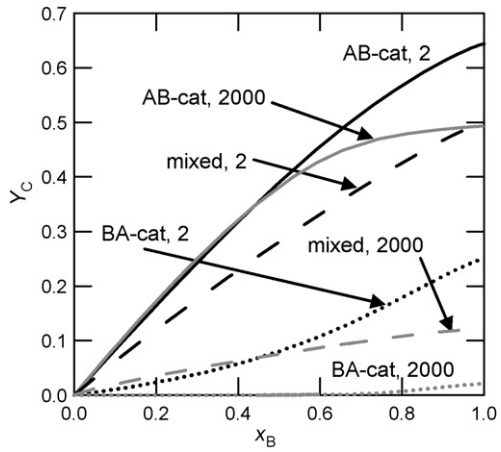

Fig. 11. Effects of fluid segment size on Y_C in the irreversible parallel reactions. The numbers after the name of the configuration indicate the channel size in micrometers.

3.3. Effects of fluid segment size

Fig. 11 shows the effects of fluid segment size on the yield of C for each configuration. For all configurations examined, Y_C increased with reducing W. Configuration AB-cat gives high Y_C even at $W = 2000\ \mu m$. For configuration mixed, the channel of $W = 2\ \mu m$ is necessary to achieve comparable Y_C of configuration AB-cat of $W = 2000\ \mu m$ at $x_B = 1.0$. This result indicates that proper design of fluid segment configuration is more effective than reducing channel width to improve the yield and selectivity of the desired product for diffusion-controlled catalytic surface reactions. Avoiding smaller channel sizes than necessary is also desirable from the viewpoint of pressure drop in the channel.

4. Conclusions

We investigated the effects of the configuration of fluid segments including reactants at the reactor inlet for catalytic surface reactions in microreactors. We applied irreversible and reversible parallel and series–parallel reaction systems in the channel between two parallel plates in CFD simulations. We also examined the effects of the following rate-controlling steps of the reaction systems: diffusion in the channel or diffusion in the catalyst layer. Under diffusion-controlled conditions, a proper fluid segment configuration results in higher selectivity of the desired product than where the reactants are mixed at the reactor inlet. The configurations in which reactants with reactions of different orders in parallel reactions or consumed only in the reaction producing the desired product are placed near the catalyst surface improve the selectivity of the desired product. The arrangement to maximize the desired product yield and selectivity depends on the reaction system and rate-controlling step. For parallel reactions, the configuration in which a reactant with higher reaction orders for the reaction producing the desired product is placed on the catalyst surface improves the selectivity of the desired product. To enhance the selectivity for series–parallel reactions, the reactant consuming the desired product as well as producing it should be separated from the catalyst surface. When each parallel reaction takes place in different parts of the catalyst layer, and the reaction producing the desired product occurs at the bottom of the catalyst layer, the configuration in which reactants are mixed at the reactor inlet gives the highest product selectivity. To obtain a given degree of selectivity of the desired product, the required fluid segment size can differ by three orders of magnitude with fluid segment configuration. Proper configuration allows channel sizes smaller than necessary to be avoided. The results described here indicate the advantage of fluid segment, which is a typical fluid operation in microreactors, to enhance the yield and selectivity of the desired products.

Acknowledgment

This research was conducted as part of the Project of Micro-Chemical Technology for Production, Analysis, and Measurement Systems supported financially by the New Energy and Industrial Technology Development Organization (NEDO).

References

[1] K.F. Jensen, Microreaction engineering—is smaller better? Chem. Eng. J. 56 (2001) 293–303.
[2] V. Hessel, S. Hardt, H. Löwe, Chemical Micro Process Engineering, Wiley-VCH, Weinheim, Germany, 2004.
[3] E.V. Rebrov, S.A. Duinkerke, M.H.J.M. de Croon, J.C. Schouten, Optimization of heat transfer characteristics, flow distribution, and reaction processing for a microstructured reactor/heat-exchanger for optimal performance in platinum catalyzed ammonia oxidation, Chem. Eng. J. 93 (2003) 201–216.
[4] R. Gorges, S. Meyer, G. Kreisel, Photocatalysis in microreactors, J. Photochem. Photobiol., A 167 (2004) 95–99.
[5] A. Karim, J. Bravo, D. Gorm, T. Conant, A. Datye, Comparison of wall-coated and packed-bed reactors for steam reforming of methanol, Catal. Today 110 (2005) 86–91.
[6] Z. Ni, E.G. Seebauer, R.I. Masel, Effects of microreactor geometry on performance: differences between posted reactors and channel reactors, Ind. Eng. Chem. Res. 44 (2005) 4267–4271.
[7] L. Kiwi-Minsker, A. Renken, Microstructured reactors for catalytic reactions, Catal. Today 110 (2005) 2–10.
[8] Y.S.S. Wan, J.L.H. Chau, K.L. Yeung, A. Gavriilidis, 1-Pentene epoxidation in catalytic microfabricated reactors, J. Catal. 223 (2004) 241–249.
[9] Z. Xu, Y. Ju, Concentration slip andits impact on heterogeneous combustion in a micro scale chemical reactor, Chem. Eng. Sci. 60 (2005) 3561–3572.
[10] T. Gervais, K.F. Jensen, Mass transport and surface reactions in microfluidic systems, Chem. Eng. Sci. 61 (2006) 1102–1121.
[11] W. Ehrfeld, K. Golbig, V. Hessel, H. Löwe, T. Richter, Characterization of mixing in micromixers by a test reaction: single mixing units and mixer arrays, Ind. Eng. Chem. Res. 38 (1999) 1075–1082.
[12] St. Ehlers, K. Elgeti, T. Menzel, G. Wieβmeier, Mixing in the offstream of a microchannel system, Chem. Eng. Proc. 39 (2000) 291–298.
[13] P. Löb, K.S. Drese, V. Hessel, S. Hardt, C. Hofmann, H. Löwe, R. Schenk, F. Schönfeld, B. Werner, Steering of liquid mixing speed in interdigital micro mixers—from very fast to deliberately slow mixing, Chem. Eng. Technol. 27 (2004) 340–345.
[14] H. Nagasawa, N. Aoki, K. Mae, Design of a new micromixer for instant mixing based on collision of micro segment, Chem. Eng. Technol. 28 (2005) 324–330.
[15] N. Aoki, K. Mae, Effects of channel geometry on mixing performance using collision of fluid segments, Chem. Eng. J. 118 (2006) 189–197.
[16] N. Daito, N. Aoki, J. Yoshida, K. Mae, Selective condensation reaction of phenols and hydroxybenzyl alcohol using micromixers based on collision of fluid segments, Ind. Eng. Chem. Res. 45 (2006) 4954–4961.

[17] N. Aoki, S. Hasebe, K. Mae, Mixing in microreactors: effectiveness of lamination segments as a form of feed on product distribution for multiple reactions, Chem. Eng. J. 101 (2004) 323–331.
[18] N. Aoki, S. Hasebe, K. Mae, Geometric design of fluid segments in microreactors using dimensionless numbers, AIChE J. 52 (2006) 1502–1515.
[19] N. Aoki, K. Mae, Improvement of product yield and selectivity in microreactors by combining fluid segments of different concentrations and sizes, Stud. Surf. Sci. Catal. 159 (2006) 641–644.
[20] Fluent 6.2 User's Guide, Fluent Inc., Lebanon, USA, 2005, Chapter 26.
[21] H.S. Fogler, Elements of Chemical Reaction Engineering, 4th ed., Pearson Education, Upper Saddle River, USA, 2005, p. 770.
[22] T. Maki, T. Ueyama, K. Mae, Methanol decomposition by the use of an assemble-type microreactor, Chem. Eng. Technol. 28 (2005) 494–500.
[23] J. Yoshida, A. Nagaki, T. Iwasaki, S. Suga, Enhancement of chemical selectivity by microreactors, Chem. Eng. Technol. 28 (2005) 259–266.
[24] O. Levenspiel, Chemical Reaction Engineering, 3rd ed., John Wiley & Sons, New York, USA, 1998, pp. 314–315.
[25] A. Tuel, S. Moussa-Khouzami, Y.B. Taarit, C. Naccache, Hydroxylation of phenol over TS-1: surface and solvent effects, J. Mol. Catal. 68 (1991) 45–52.